AAPS PharmSciTech, Vol. 14, No. 2, June 2013 (© 2013)
DOI: 10.1208/s12249-013-9949-x

Research Article

Formulation and Development of Extended-Release Micro Particulate Drug Delivery System of Solubilized Rifaximin

Rohan V. Karanje,[1] Yogita V. Bhavsar,[1] Kirti H. Jahagirdar,[1] and Kiran S. Bhise[1,2]

Received 2 September 2012; accepted 25 February 2013; published online 21 March 2013

Abstract. Rifaximin (RFX), a semi-synthetic antibiotic belonging to BCS class IV category, has been used in the treatment of traveler's diarrhea. An attempt has been made to improve aqueous solubility of RFX in the presence of β-cyclodextrin (β-CD) and hydroxy propyl β-cyclodextrin (HP-β-CD) and control its release in the gut by enteric coating. The stoichiometric proportion of RFX and complexing agent's β-CD and HP-β-CD were determined by phase solubility studies. RFX–β-CD and RFX–HP-β-CD were prepared in 1:2 ratio by solvent evaporation technique using rota-evaporator with yield of 78% and 84% respectively followed by their evaluation using different techniques such as saturation solubility, Fourier transform infrared, differential scanning calorimeter, powder X-ray diffractometer, *in vitro* antimicrobial activity. The saturation solubility of RFX had improved from 0.0736 mg/ml to 0.2354 mg/ml and 0.5681 mg/ml in presence of β-CD and HP-β-CD respectively resulting in an increased zone of inhibition in the later complex during antimicrobial studies. The RFX–HP-β-CD complex particles were coated with eudragit L 100 (EL 100) by spray drying technique. The 3^2 factorial design was applied to formulate the micro particles. All formulations exhibited pH dependant drug release. The % EE was 69% and the release of RFX was retarded by enteric coating in the optimized batch FB2. Therefore, it can be concluded that solubility of some BCS class IV drugs can be improved by β-CD complexation and release of such inclusion complexes can be retarded to increase the residence time of RFX in the gastrointestinal tract.

KEY WORD: cyclodextrin complexes; eudragit L 100; micro particles; rifaximin; spray dryer.

INTRODUCTION

Most of the drugs currently marketed are semi-synthetic or synthetic in nature. However, these molecules suffer from several disadvantages including very low solubility, poor permeability, toxicity etc. Rifaximin (RFX) 5,6,21,23,25-entahydroxy-27-methoxy-2,4,11,16,20,22,24,26-octamethyl-2,7-(epoxypentadeca-[1,11,13]trienimino) benzofuro [4,5-*e*] pyrido[1,2-*a*]-benzimida-zole-1,15(2*H*)-dione,25-acetate (1), empirical formula, $C_{43}H_{51}N_3O_{11}$, a BCS class IV, an orphan drug, is used against traveler's diarrhea. The dosing interval of RFX is thrice a day of which 96.62% is excreted in feces almost entirely as unchanged drug. The current literature survey reveals its usage in the controlled drug delivery system (2–4) to increase the residence time of RFX in the gastrointestinal tract. The aqueous solubility of RFX has been improved by usage of bile salts (5,6). The literature survey reveals that no significant work has been reported in improving aqueous solubility of RFX. Cyclodextrins (CD) are cyclic oligosaccharides made up of six to eight D-glucose monomers connected at one and four carbon atoms with a hydrophilic outer surface and lipophilic central cavity to which the lipophilic drug binds and protects itself from an aqueous environment thereby enhancing its solubility. Cyclodextrin complexation provides molecular shielding by encapsulating labile drugs molecules at molecular level and protects them against various degradation processes and increase the shelf life of drugs. Research conducted in last few decades on CDs and its derivatives such as hydroxy propyl β cyclodextrin (HP-β-CD) has demonstrated wide use in improving the aqueous solubility of drugs (7). The scientific discussion on RFX reveals that as its concentration increases in gut, better results have been achieved against traveler's diarrhea. In the present work, an attempt has been made to improve an aqueous solubility of RFX with an aid of beta-cyclodextrin (β-CD) and HP-β-CD, respectively and controlling RFX release in gut by enteric coating. The complexes were prepared with an aid of a rotary evaporator. The complexes were prepared and were further enteric-coated by eudragit L 100(EL 100) with an aid of spray drying technique.

[1] Department Of Pharmaceutics, MCE Society's Allana College of Pharmacy, Azam Campus, Camp Pune, 411001 Maharashtra, India.
[2] To whom correspondence should be addressed. (e-mail: principalacpharm@azamcampus.org)

ABBREVIATIONS: ANOVA, Analysis of variance; β-CD, Beta-cyclodextrin; BCS, Biopharmaceutical classification system; R, Coefficient of correlation; °C, Degree Celsius; % DR, Percentage drug release; DSC, Differential scanning calorimeter; % EE, Percentage entrapment efficiency; EL 100, eudragit L 100; HP-β-CD, Hydroxy propyl β cyclodextrin; mm, Millimeter; mg, Milligram; ml, Milliliter; PBS pH6.8, Phosphate buffer solution pH6.8; PXRD, Powder X-ray diffractometer; *P*, Probability; RFX, Rifaximin; rpm, Revolution per minute; SEM, Scanning electron microscopy; USP, United state pharmacopeia.

MATERIALS

RFX was procured from Sigma Aldrich, β-CD was purchased from Hi-media Lab, Mumbai; HP-β-CD, EL 100 and Methanol were purchased from Loba Chemie. The rest of the chemicals were of analytical grade.

METHOD

Phase solubility Study (8–13)

In order to determine complexing ratio of RFX and CD, phase solubility study was performed by adding increasing molar concentration of β-CD in linear proportion to drug solution. An excess quantity of RFX was added separately to 20 ml of solutions of β-CD in the concentration ranges from 0.002 to 0.012 M in clean and dry calibrated 100 ml volumetric flasks, followed by constant stirring on an orbital linear shaker (150 rpm) for 24 h at room temperature (25°C). Accurately measured 10-ml aliquots were withdrawn in triplicate from each volumetric flask after 24 h. The aliquots were then filtered and assayed for RFX at 436 nm. The procedure was repeated to carry out phase solubility for HP-β-CD in the concentration range of 0.002 to 0.014 M.

Preparation of the Inclusion Complexes

The complexes were prepared by solvent evaporation technique. An accurately weighed 144 mg of RFX was mixed with 288 mg of β-CD to obtain the drug polymer ratio of 1:2. The mixture was placed in methanol–water system (9:1) with continuous stirring on linear motion shaker (Spectra lab Whirlmatic, Mumbai; Model No.TH100) for about 24 h. The inclusion complex was obtained as dry powder by evaporating the solvent at a temperature above 70°C or sufficient to evaporate water using rotary evaporator and the complexes were collected, weighed, stored in glass vial and dried at room temperature. The same procedure was adopted to prepare HP-β-CD complexes. The complexes were subjected for characterization.

Preparation of Trial Batches of Microparticles (14–19)

Accurately weighed 500 mg of RFX and 1,000 mg of HP-β-CD were mixed in methanol–water (9:1) solvent system with constant stirring for 24 h with an addition of EL 100 solution in the concentration ranging from 0.5 to 2% *w/v*. The solutions were constant stirred under ultraturrax (Model No—EN 30US, IKA) at 15,000 rpm for 15 min, and were subjected to spray drying at vacuum pressure of 40, 80, 120 (−mm/Wc). Twelve such trial batches were formulated.

3^2 Full Factorial Design (17–20)

The effect of formulation variables on the responses were statistically evaluated by applying one-way ANOVA at 0.05 level, using the commercially available software package Design-Expert®, version 8.0. The 3^2 factorial design was implemented for optimization of microparticles that contained two independent variables at three levels +1, 0 and −1 as depicted in Table I. The three levels were decided on the basis of trial batches and their evaluation. The difference between two consecutive levels was maintained constant and accordingly total nine formulations were designed. The different independent variables include EL 100 concentration (X_1) and vacuum pressure (X_2). The batches were evaluated and the effect of individual variable was studied according to the response surface methodology. The different dependent responses include: % EE (Y_1) and cumulative % DR at the end of the eighth hour (Y_2). To describe the response surface curvature, the design was evaluated by following quadratic equation:

$$Y = \beta_0 + \beta_1 X_1 + \beta_2 X_2 + \beta_{12} X_1 X_2 + \beta_{11} X_1^2 + \beta_{22} X_2^2 \quad (1)$$

Where

Y	Response variable
β_0	Constant
$\beta_1 \ldots \beta_{22}$	Regression coefficient
X_1 and X_2	Main effect
X_1X_2	Interaction terms; show how response changes when two factors are simultaneously changed.

Formulation of the Optimized Batch

The optimized batch (FB2) was formulated using the predicted values of EL 100 concentration and vacuum from the software.

Evaluation of Complexes

The inclusion complexes of RFX–β-CD and RFX–HP-β-CD were evaluated for the following studies:

Saturation Solubility (10–12)

The saturated solubility of pure RFX, RFX–β-CD, and RFX–HP-β-CD complexes were determined in distilled water (DW) and phosphate buffer solution pH6.8 (PBS pH6.8)by dissolving an excess amount (100 mg) of the samples separately in 100 ml solution of medium A (90 ml of DW and 10 ml of 1.5% sodium lauryl sulfate, i.e., SLS) with constant stirring on linear motion shaker (Spectra lab Whirlmatic; Model No.TH100) for 24 h till the attainment of equilibrium followed by filtration and

Table I. Levels of Variables in Coded and Actual Form

	Actual values		Response	
Levels (code value)	X_1 (−vacuum)	X_2 (% *w/v*) (EL 100)	Y_1	Y_2
−1	40	1.25	% Entrapment efficiency	% Drug release
0	80	1.50		
+1	120	1.75		

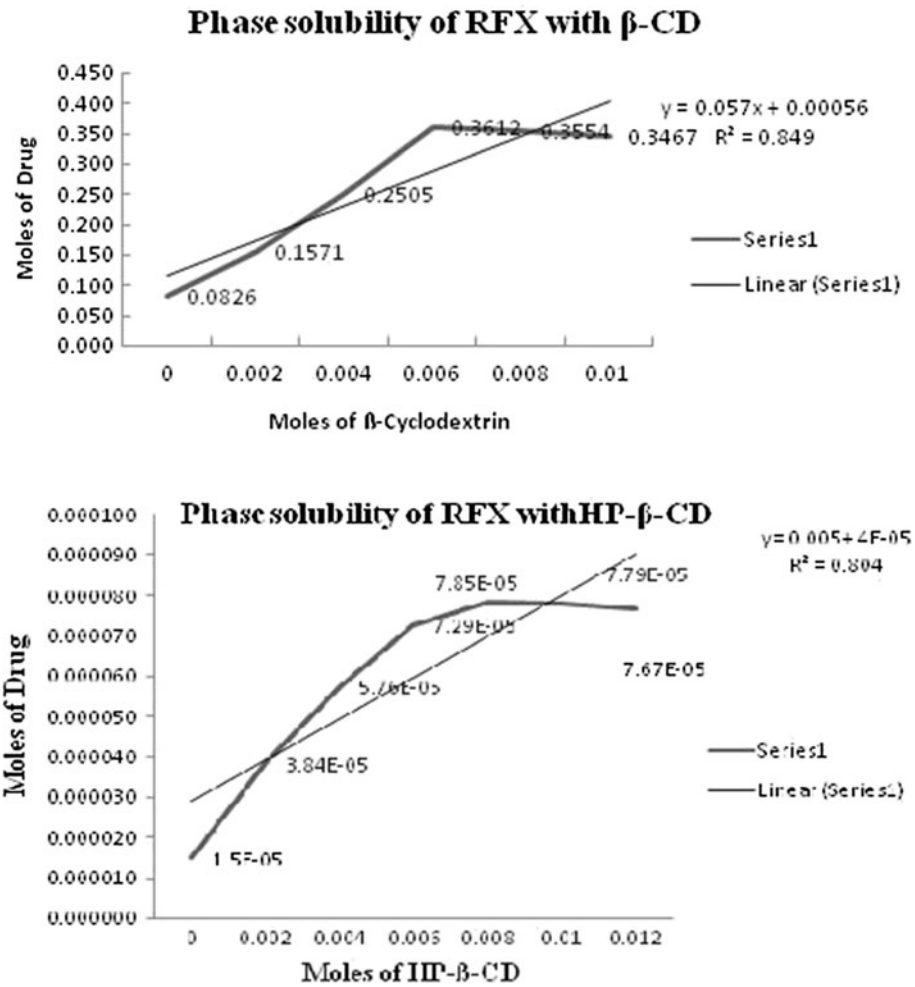

Fig. 1. Phase solubility for RFX with β-CD and HP-β-CD

UV visible spectroscopic estimation at 436 nm and 437.8 nm for DW and PBS pH6.8, respectively, on UV visible spectrophotometer (Jasco V-630).

Fourier Transform Infrared Spectrometry

Fourier transform infrared (FTIR) spectra of the samples of pure drug RFX, β-CD and HP-β-CD complexes were recorded on FTIR spectrometer (Model No-FT/IR-4100 Jasco Corporation Tokyo, Japan) for the purpose of characterization. The samples were mixed with potassium bromide in 1:10 ratio to obtain spectra in the range 500–4,000 cm^{-1}.

In Vitro Antimicrobial Activity (13)

Accurately weighed 10 mg of RFX was added to 100 ml DW with constant stirring at 100 rpm for 24 h to get 100 μg/ml solution. Accurately weighed RFX–β-CD and RFX–HP-β-CD complexes (1:2) each equivalent to 10 mg of RFX was added to DW with constant stirring at 100 rpm for 24 h to get 100 μg/ml solution. The zone of inhibition of RFX and inclusion complexes were determined by placing a bore in sterilized petri plates with help of sterilized bore former. Accurately measured 100 μL of the RFX, RFX–β-CD, and RFX–HP-β-CD solutions were poured in the well of respectively labeled plates that were incubated for 24 h and the zone of inhibition for all the samples were determined in triplicate to minimize the error.

Table II. Phase Solubility Analysis Data for RFX with β-CD and HP-β-CD

Moles of β-CD	Concentration of RFX (μg/ml)	Moles of drug	Moles of HP-β-CD	Concentration of RFX (μg/ml)	Moles of Drug
0	5.41	0.0826	0	6.097	0.000015
0.002	10.492	0.1571	0.002	17.18	0.0000384
0.004	16.609	0.2505	0.004	25.62	0.0000576
0.006	23.86	0.3612	0.006	28.65	0.0000729
0.008	23.48	0.3554	0.008	30.85	0.0000785
0.01	22.91	0.3467	0.01	29.55	0.0000779
–	–	–	0.012	28.13	0.0000767

Table III. Process Parameters and Evaluation of Trial Batches for % yield, %EE and Cumulative % DR of Trial Batches

Batch code	Drug (mg)	HP-β-CD (mg)	EL 100 (%)	Vacuum (−mm/Wc)	Inlet temp. (°C)	Feed pump rate(ml/h)	% yield	% EE[a]	Cumulative % DR[a]
A1	500	1,000	0.5	40	70	40	31.56	48.44±2.12	85.083±0.05
A2	500	1,000	0.5	80	70	40	18.95	31.40±2.63	89.8305±0.08
A3	500	1,000	0.5	120	70	40	11.32	19.71±0.48	98.393±0.16
B1	500	1,000	1.0	40	70	40	33.16	59.51±0.05	89.356±0.35
B2	500	1,000	1.0	80	70	40	22.68	45.84±0.12	93.495±0.46
B3	500	1,000	1.0	120	70	40	15.80	33.26±0.68	98.401±0.14
C1	500	1,000	1.5	40	70	40	35.44	78.19±0.12	70.589±0.06
C2	500	1,000	1.5	80	70	40	26.37	69.83±0.25	77.691±0.12
C3	500	1,000	1.5	120	70	40	16.85	60.71±0.36	85.492±0.06
D1	500	1,000	2.0	40	70	40	41.64	108.67±0.01	46.008±0.17
D2	500	1,000	2.0	80	70	40	37.08	98.33±0.32	52.287±0.09
D3	500	1,000	2.0	120	70	40	31.95	93.14±0.28	58.682±0.07

[a] Data represents n=3, mean±SD

Differential Scanning Calorimetry

The thermal behaviors of pure drug RFX, RFX–β-CD, and RFX–HP-β-CD complex samples were examined by differential scanning calorimeter (DSC 821e, Mettler Toledo, Japan). Indium/zinc standards were used to calibrate the temperature and enthalpy scale. The samples were scanned at the heating rate of 10°C/min over a temperature range of 20 to 100°C. Peak transitions and enthalpy of fusion were determined for the samples using TA 60 integration software.

X-Ray Powder Diffraction

RFX–β-CD and RFX–HP-β-CD complexes were subjected to powder X-ray diffraction (PXRD) using X-Ray Generator, Bruker Axis, D8 Advance, Germany. To study X-ray diffraction pattern, the samples were placed into aluminum holder and the instrument was operated between initial and final 2θ angle of 5–50° respectively in an increment of 0.1^0 2θ.

Evaluation of Microparticles (14–19)

The microparticles were evaluated for the following studies:

Percentage Entrapment Efficiency (% EE)

Accurately weighed 100 mg of microparticles of RFX were added to 100 ml of medium A with constant stirring on linear motion shaker (Spectra lab Whirlmatic; Model No TH100) for 24 h followed by centrifugation at 11,000 rpm for 30 min. The undissolved particles in the solution were removed by filtration through Whatman filter paper no. 40. The drug concentration was estimated at 436 nm in triplicate on UV visible spectrophotometer (Jasco V-630). The % EE was calculated as per the formula:

$$\% \text{ EE} = \frac{\text{Practical drug content}}{\text{Theoretical drug content}} \times 100 \qquad (2)$$

Cumulative % Drug Release (% DR)

In vitro cumulative % DR was performed using USP NF XIII Type I (basket type) model. The dissolution for each batch was carried out by loading microparticles equivalent to 200 mg of RFX in six capsules each of size 000 and performing dissolution for 2 h in 900 ml medium B (0.1 N HCl and 10 ml of 1.5% SLS) followed by dissolution in 900 ml medium C (PBS pH6.8 and 10 ml of 1.5% SLS) for further 8 h. The temperature was maintained at 37±0.5°C and at a constant rotation speed of 100 rpm. Samples were withdrawn at 1 h intervals maintaining sink condition. They were analyzed by UV–Visible spectrophotometer (Jasco, V630) at 437.4 and 437.8 nm, respectively, with suitable dilutions and the readings were taken in triplicate.

Table IV. Process Parameters and Evaluation of Factorial Batches FA1 - FC3

Batch code	RFX (mg)	HP-β-CD (mg)	EL 100 (%) (X_1)	Vacuum (X_2) (−mm/Wc)	% EE[a]	Cumulative % DR
FA1	500	1,000	1.25	40	71.265±0.101	77.13±0.06
FA2	500	1,000	1.25	80	60.322±0.14	85.345±0.62
FA3	500	1,000	1.25	120	45.058±0.022	97.705±0.062
FB1	500	1,000	1.5	40	78.036±0.567	70.513±0.57
FB2	500	1,000	1.5	80	69.014±0.005	77.668±0.039
FB3	500	1,000	1.5	120	60.116±0.063	85.458±0.93
FC1	500	1,000	1.75	40	95.764±0.131	55.479±0.88
FC2	500	1,000	1.75	80	89.229±0.085	63.288±0.355
FC3	500	1,000	1.75	120	84.095±0.194	69.708±0.093

[a] Data represents n=3, mean±SD

Evaluation of Optimized Batch (FB2)

The evaluation of the optimized batch FB2 was performed by the above parameters.

Scanning Electron Microscopy

The shape and surface morphology of the optimized batch FB2 of enteric-coated RFX microparticles were investigated using scanning electron microscopy (SEM). The samples were prepared by sprinkling the formulation on double adhesive tape stuck to aluminum stub. The stub was placed in high vacuum evaporator. The samples were then randomly scanned and photomicrographs were taken with a scanning electron microscope (Joel JSM-630A, Tokyo, Japan).

Accelerated Stability Study

During stability studies, the product was exposed to conditions of temperature and humidity as per ICH guidelines. The microparticles were sealed in an aluminum packaging coated inside with polyethylene at a temperature of 40°C±2°C and 75±5% RH for duration of 3 months. The stability of sample maintained after an interval of every 1 month was tested for Cumulative % DR study.

RESULTS AND DISCUSSION

Phase Solubility Studies

In order to decide the stoichiometric proportion of RFX and complexing agents β-CD and HP-β-CD, phase solubility study was performed. The results have been demonstrated in Fig. 1 and Table II. The data reveals an improvement in the aqueous solubility of RFX with an increase in concentration of β-CD and HP-β-CD in a linear fashion up to maximum level followed by a slight decrease in solubility. The phase solubility plot demonstrates solubility curve for both β-CD and HP-β-CD, revealing formation of 1:2 RFX–β-CD and RFX–HP-β-CD inclusion complexes. The apparent stability constant ($K_{1:2}$) for the RFX: β-CD and RFX: HP-β-CD complexes were 105.23 and 131.51 M^{-1} respectively. It was observed that RFX had limited stability in methanol and the drug was degraded upon its storage in methanol for few hours. It was seen that RFX complexation with β-CD stabilized the drug for

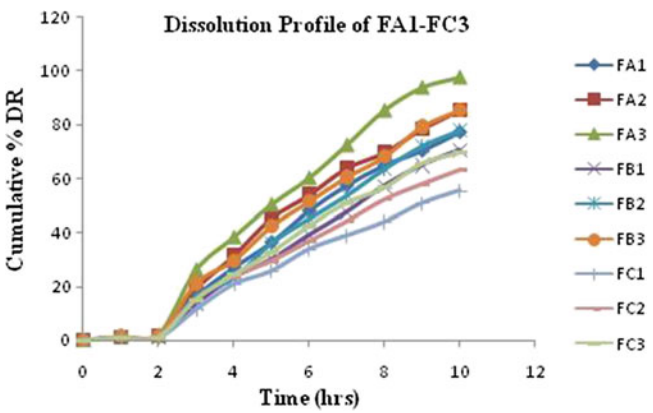

Fig. 2. Dissolution profile of factorial batches FA1–FC3

Table V. Data for Release Exponent of Factorial Batches of RFX Micro Particles Prepared as Per 3^2 Factorial Design

	Parameter	
Batch code	% DR at 8 h	Release exponent (*n*)
FA1	77.13±0.06	0.6608
FA2	85.345±0.62	0.7108
FA3	97.705±0.06	0.6942
FB1	70.513±0.57	0.7469
FB2	77.668±0.03	0.6917
FB3	85.458±0.93	0.7652
FC1	55.479±0.88	0.7502
FC2	63.288±0.35	0.7617
FC3	69.708±0.09	0.8084

weeks, assuring its stability in methanol. The complexes exhibited good stability constant ensuring that the subsequent release of RFX would not take place in the

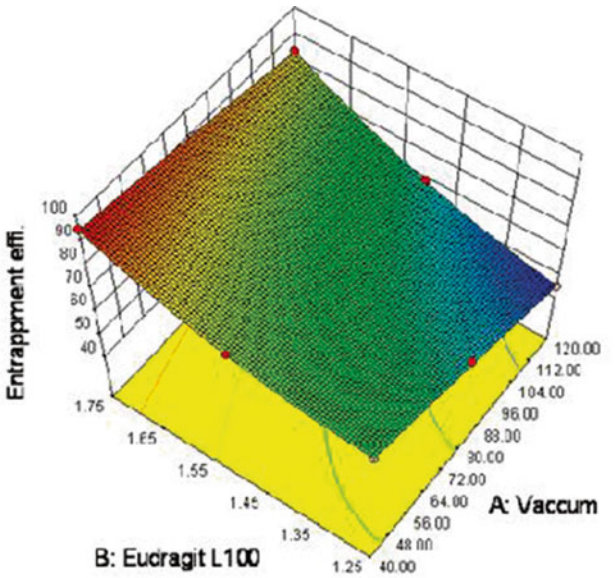

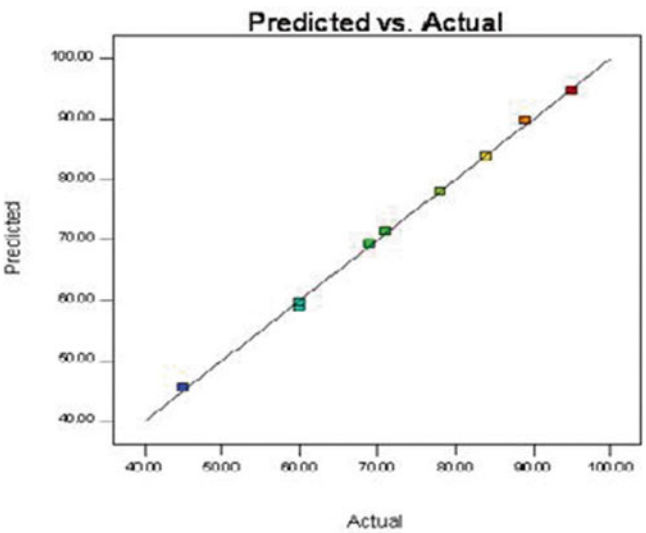

Fig. 3. Response surface plot and predicted *vs.* actual graph for % EE

coating solution containing only methanol and EL 100. The inclusion complex of RFX–β-CD and RFX–HP-β-CD were prepared by solvent evaporator using rota-evaporator with a yield of 78% and 84%, respectively.

Effect of Vacuum Pressure and Polymer Concentrations

It is quite evident from the data depicted in Table III that with an increase in vacuum pressure, % yield and % EE has decreased; whereas an increase in the concentration of EL 100 from 0.5 to 2%, there was an improvement in the % EE. This was due to the fact that at low vacuum rate particles remained in the chamber causing them to interact with more polymer and thereby increasing the coating of particles and hence % EE. It was found that batches A and B with 0.5 and 1.0% EL100 exhibited poor % EE due to low concentration of polymer. The batches A, B, C, and D presented % EE of 48, 59, 78.19, and 108.67 respectively at vacuum 40 mm/Wc. As % EE was decreased, a significant effect on drug release was noted. An increase in polymer concentration resulted in retardation of % DR. The batches A1 to A3 exhibited poor drug entrapment with %DR of RFX in 6 h. Similarly, batches B1 to B3 showed better entrapment than batch A but the release was prolonged to 7 h due to an increase in polymer concentration. Batches C1 to C3 and D1 to D3 demonstrated good entrapment of RFX with drug release extended to 8 h. Amongst all the formulations, batch C2 exhibited desired results of 69.83% EE and 77% cumulative drug release. The batch exhibiting 65–75% EE and 70–80% DR was chosen for factorial design. The results of % EE and % DR have been depicted in Table IV. Figure 2 indicates that the FA3 shows drug release 97.705±0.062, and FC1 exhibited lowest drug release 55.479±0.88 in 8 h. The best fit model was found to be the Korsmeyer–Peppas as per R value. The values of diffusion exponent are as indicated in Table V were found to be in the range of 0.6914–0.8084. Factorial formulations exhibited anomalous or non-Fickian type drug release controlled by swelling, diffusion of drug, that is combination of both diffusion and erosion controlled release followed by polymer chains relaxation. The release profile clearly indicates an increase in core/coat ratio leading to retardation of drug release. The Quadratic model for % EE was found to be significant with an F value 501.91 ($P<0.0001$). In this case X_1, X_2, X_1X_2 was found to be significant and the model describes the % EE. The factorial equation for % EE (Y_1) was:

$$Y_1 = 69.33 - 9.17X_1 + 15.33X_2 + 3.75X_1X_2 - 0.50X_1^2 + 5.00X_2^2 \quad (3)$$

The vacuum (factor X_1) has a negative effect whereas concentration of EL 100 (factor X_2) exerts positive effect on % EE (Y_1). The combined effect of X_1 and X_2 indicates significant effect on % EE. Figure 3 presents the response surface plot and correlates the values of predicted and the actual observation. The response surface plot indicates that for 90% of % EE, concentration of EL100 and vacuum should be in the range of 1.65–1.75 and 75–85. FB2 was selected as the optimized batch for further studies based upon its release profile. The predicted *vs*. actual values graph indicates a proportionate increase in entrapment as all the values are on the same line. For 70% of % EE, the predicted value is 69% indicating correlation between the actual and predicted values. The Quadratic model for % DR was found to be significant with F value 14.65 ($P<0.0256$). In this case X_1, X_2, X_1X_2 was found to be significant and the model describes the % DR. The factorial equation for % DR at 8 h (Y_2) was:

$$Y_2 = 77 + 3.50X_1 - 12.00X_2 - 8.50X_1X_2 + 0.501X_1^{2-}3.00X_2^2 \quad (4)$$

The equation presents a positive effect of vacuum (factor X_1) whereas concentration of EL 100 (factor X_2) has negative effect on the cumulative % drug release. The combined effect of X_1 and X_2 indicates significant effect on the cumulative % drug release. Figure 4 presents the response surface plot and correlates the values of predicted and the actual observation of % DR. The response surface plot indicates that for 80% of % DR the concentration of EL100 and vacuum should be in the range of 1.35–1.65 and 65–85. For 80% of % DR, the predicted value is 79% which is close to the release profile of FB2 batch.

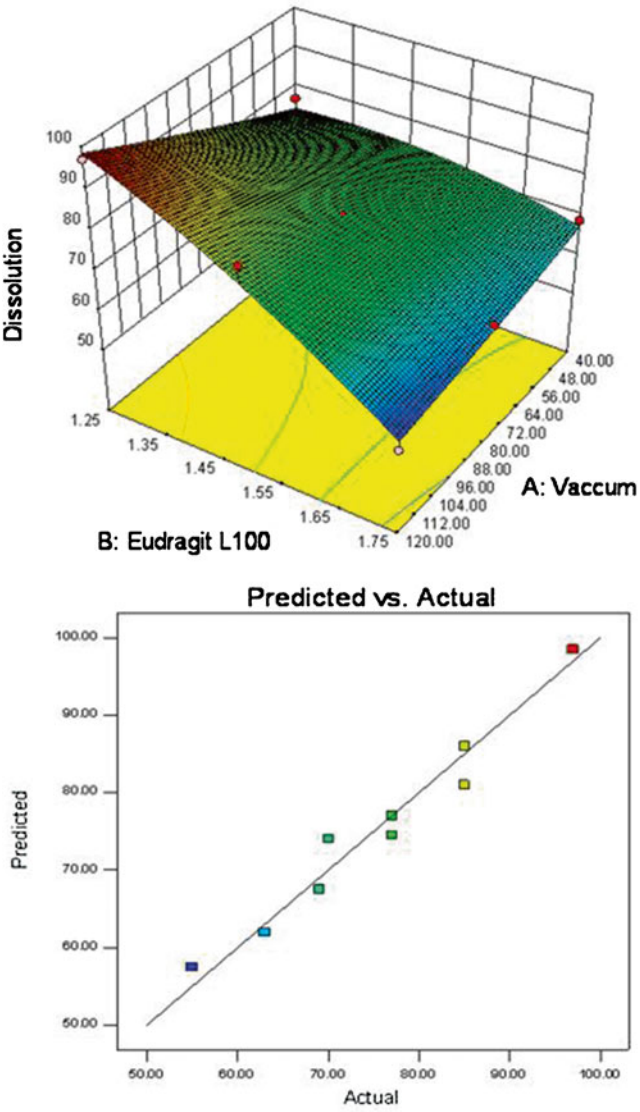

Fig. 4. Response surface plot and predicted *vs*. actual graph for % DR

Table VI. FTIR Spectra

Functional groups	RFX peaks (cm^{-1})	β-CD peaks (cm^{-1})	HP-β-CD peaks (cm^{-1})	EL 100 peaks (cm^{-1})	RFX–β-CD peaks (cm^{-1})	RFX–HP-β-CD peaks (cm^{-1})	RFX–HP-β-CD-EL 100 peaks (cm^{-1})
–OH group stretching	3,423 cm^{-1}	3,371 cm^{-1}	3,424 cm^{-1}	3,424 cm^{-1}	3,400 cm^{-1}	3,400 cm^{-1}	3,400 cm^{-1}
Free –OH group	–	–	3,611 cm^{-1}		3,600 cm^{-1}	3,600 cm^{-1}	3,626 cm^{-1}
Ketone group	1,723 cm^{-1}	–	–	1,730 cm^{-1}	1,723 cm^{-1}	1,723 cm^{-1}	1,723 cm^{-1}
Ester linkages	1,651 cm^{-1}	1,543 cm^{-1}	–	1,705 cm^{-1}	1,651 cm^{-1}	1,651 cm^{-1}	–
Pyrrole ring	1,570 cm^{-1}	1,543 cm^{-1}	–	–	1,570 cm^{-1}	1,570 cm^{-1}	1,527 cm^{-1}
C–H stretching	2,977 cm^{-1}	2,910 cm^{-1}	2,903 cm^{-1}	–	2,900 cm^{-1}	2,900 cm^{-1}	2,900 cm^{-1}
C–C stretch	2,877 cm^{-1}	1,448 cm^{-1}	–	1,450 cm^{-1} –1,485 cm^{-1}	1,448 cm^{-1}	1,448 cm^{-1}	–
C–H Bending	–	1,029 cm^{-1} and 1,152 cm^{-1}	1,031 cm^{-1}	–		–	–

Saturated Solubility

The saturation solubility of RFX–β-CD and RFX–HP-β-CD complexes was 0.2354 and 0.5681 mg/ml, respectively, in water, and 0.2065 and 0.5234 mg/ml, respectively, in PBS pH6.8. Drug complexation with HP-β-CD exhibited greater saturation solubility as compared to β-CD. Therefore, HP-β-CD complexes were used for enteric coating.

Fourier Transform Infrared Spectrometry

Table VI describes the FTIR spectra of RFX, β-CD, HP-β-CD, EL 100, RFX–β-CD, RFX–HP-β-CD, microparticles. RFX, β-CD, HP-β-CD, EL 100 exhibited characteristic peaks. FTIR figure prints showed superimposition of RFX, β-CD and HP-β-CD with no shift in major peaks and confirmed absence of shift and drug polymer interactions. Figure 5 demonstrates FTIR spectra of RFX, β-CD, HP-β-CD, EL 100, RFX–β-CD, RFX–HP-β-CD, microparticles. RFX characteristic peaks detected at 3,423 cm^{-1} was due to hydroxyl group; 1,723 cm−1 peak exhibited ketone group; 1,651 cm^{-1} represents ester linkages; 1,570 cm^{-1} peak was due to pyrrole ring; 2,977 cm^{-1} peak represents C–H stretching; 2,877 cm^{-1} peak indicates C–C stretch in structure. β-CD characteristic peak at 3,371 cm^{-1} was due to OH stretch; 2,910 cm^{-1} represents CH stretch in alkanes; 1,448 cm^{-1} indicates C–C stretch in ring; 1,543 cm^{-1} shows glycoside linkages; 1,029 cm^{-1} and 1,152 cm^{-1} was due to C–H bending. HP-β-CD prominent peaks at 3,424 cm^{-1} was due to OH stretching; 2,903 cm^{-1} indicates CH asymmetric stretching in aliphatic chain of HP-β-CD; 1,655 cm^{-1} shows H–O–H bending and 1,031 cm^{-1} due to C–O–C bending is observed. EL 100 characteristic peaks at 3,424 cm^{-1} was due to OH

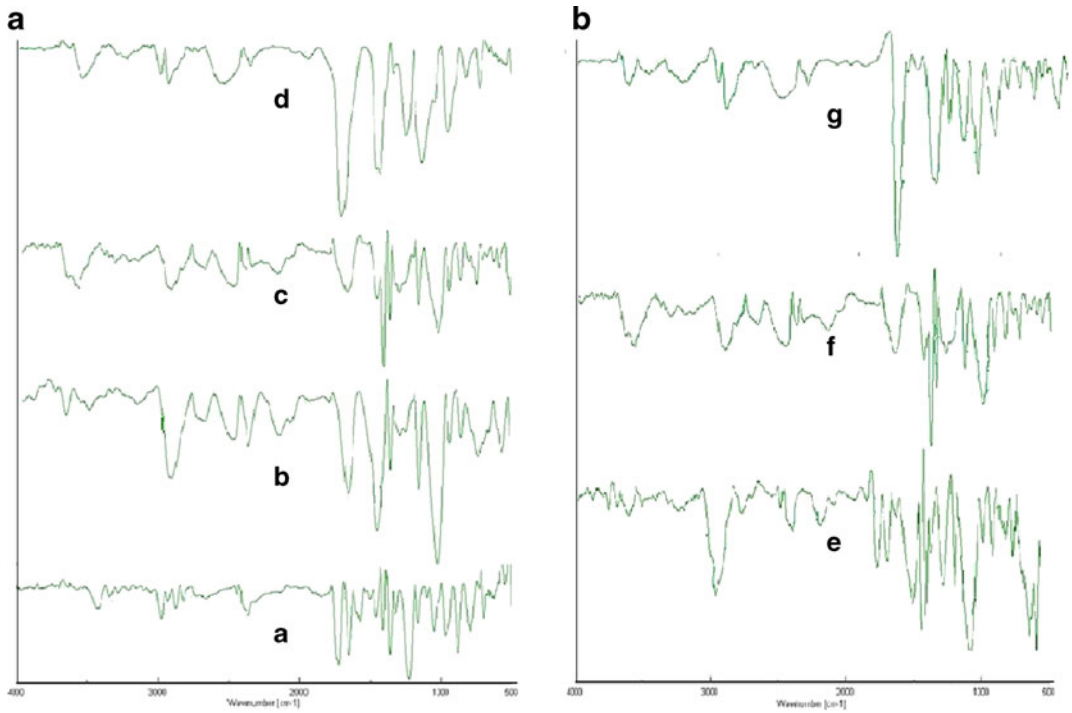

Fig. 5. **a** FTIR of (*a*) RFX, (*b*) β-CD, (*c*) HP-β-CD, (*d*) EL 100, **b** FTIR of (*e*) RFX–β-CD, (*f*) RFX–HP-β-CD, (*g*) Micro particles

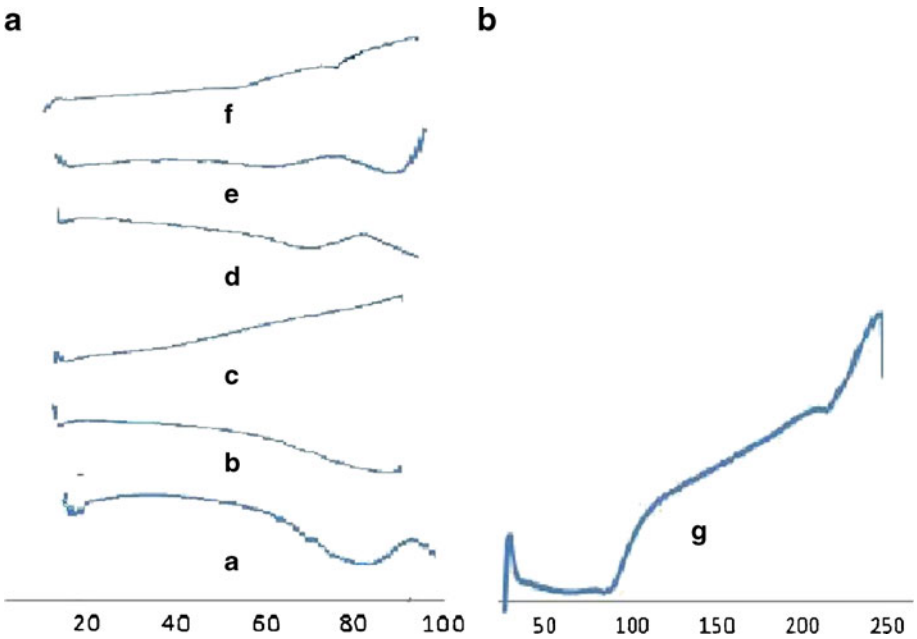

Fig. 6. **a** DSC of (*a*) β-CD, (*b*) HP-β-CD, (*c*) EL 100, (*d*) RFX–β-CD, (*e*) RFX–HP-β-CD, (*f*) Microparticles, **b** (*g*) DSC of RFX

stretching; 1,705 cm^{-1} shows carbonyl group of carboxylic acid; 1,730 cm^{-1} represents ester linkage; 1,385–1,390 cm^{-1} and 1,450–1,485 cm^{-1} indicates CH vibrations. The spectra confirmed absence of shift and drug polymer interactions.

Differential Scanning Calorimeter

The DSC of the samples were performed to check any structural interference between the polymer and the drug.

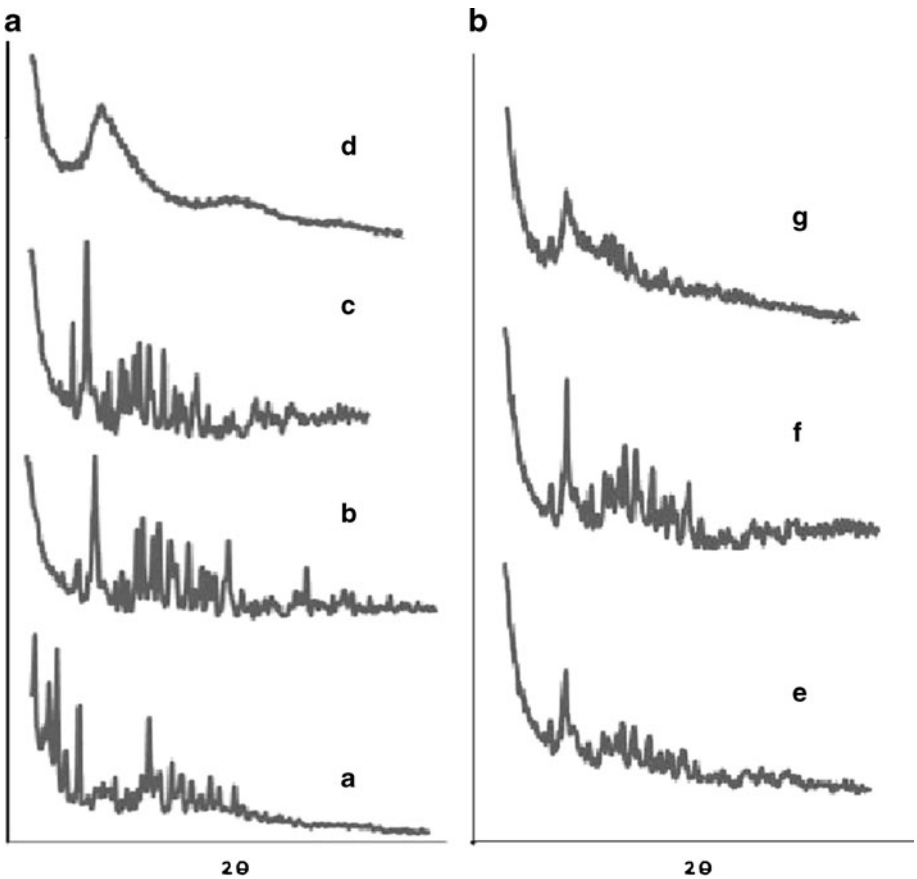

Fig. 7. **a** PXRD of (*a*) RFX, (*b*) β-CD, (*c*) HP-β-CD, (*d*) EL 100, (**b**) PXRD of (*e*) RFX–β-CD, (*f*) RFX–HP-β-CD, (*g*) micro particles

Figure 6 demonstrates DSC of RFX, β-CD, HP-β-CD, EL 100, RFX-β-CD, RFX–HP-β-CD and microparticles. DSC of RFX exhibited sharp endothermic peak at 209.31°C indicates melting point of drug. The DSC of β-CD, HP-β-CD with a very broad endothermic peak between 60°C and 90°C which attained a maximum at 75°C and 86°C, respectively, corresponds to dehydration process. EL 100 exhibited a small endothermic peak at 78°C. The DSC can be used for the recognition of inclusion complexes. When guest molecules were embedded into β-CD and HP-β-CD cavities their melting point shifted to different temperatures. The peak shifted from 209°C to 58.64°C and 68.73°C, respectively, confirming complex formation and no traces of β-CD and HP-β-CD. The microparticles showed peak at 82.14°C confirming complex coated micro particles.

Powder X-ray Diffractometer

Figure 7 depicts PXRD of RFX, β-CD, HP-β-CD, EL 100, RFX–β-CD, RFX–HP-β-CD, and microparticles. The samples RFX exhibited numerous peaks at 2θ value of 5.3, 6.9, 7.8, 10.3, and 18.3 confirming the drug to be crystalline in nature. The PXRD of β-CD exhibited characteristic peaks at 2θ values of 10.7, 12.6, 17.8, 19.6, 20.7, 22.80, and 27.2 whereas HP-β-CD exhibited characteristic peaks at 2θ values of 10.7, 12.5, 15.42, 16.98, 18.9, 20.94, and 22.80. PXRD of EL 100 presented characteristic peaks at 2θ value of 19.20. RFX–β-CD exhibited disappearance of peaks of drug whereas RFX–HP-β-CD showed decrease in intensity of characteristic peaks of the drug at 2θ values of 5.3, 6.9, 7.8, 10.3, and 18.3 microparticles exhibited single peak at 2θ value of 12.5.

Scanning Electron Microscopy

The shape and surface morphology of the optimized batch FB2 of enteric-coated RFX microparticles were investigated using SEM, the photomicrographs shown in Fig. 8 indicated the particle size in range of 1–5 μm and complete entrapment of RFX–HP-β-CD complex.

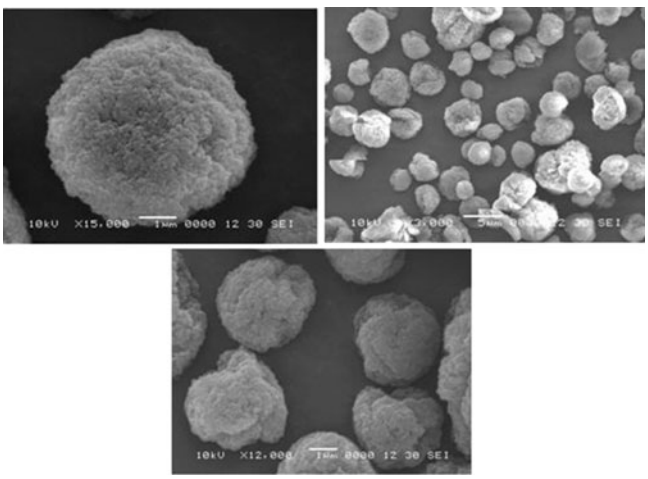

Fig. 8. SEM of optimized batch FB2

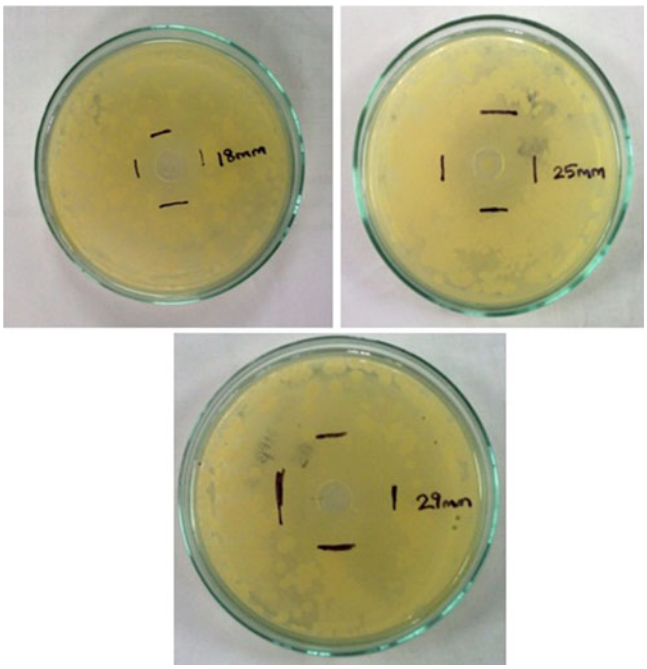

Fig. 9. *In vitro* antimicrobial activity of RFX and complexes

In vitro Antimicrobial Activity

Figure 9 exhibits zone of inhibition of RFX, RFX–β-CD, and RFX–HP-β-CD complexes by diffusion technique. Zone of inhibition of RFX was found to be 18±3.16 cm and that RFX–β-CD and RFX–HP-β-CD complexes exhibited 25±3.68 cm and 29±1.94 cm, respectively. However, the complex RFX–HP-β-CD exhibited higher zone of inhibition probably due to improved aqueous solubility of RFX in water.

The accelerated stability study performed on the optimized batch FB2 presented no change in the cumulative % drug release DR and thus the formulation can be assessed with *in vivo* activity. The authors plan to do the same in the coming days.

CONCLUSION

From the present study, it can be concluded that solubility of RFX can be improved by β-CD complexation and the drug release from such inclusion complexes can be retarded in the gastrointestinal tract by various tools.

REFERENCES

1. Martini S *et al.* Solution structure of rifaximin and its synthetic derivative rifaximin determined by experimental NMR and theoretical simulation methods. Bioorg Med Chem. 2004;12(9):2163–72. doi:10.1016/j.bmc.2004.02.027.
2. Huang DB, DuPont HL. Rifaximin—a novel antimicrobial for enteric infections. J Infect. 50(2): 97–106.
3. Jahagirdar HA. Patent Application No- 20090028940 USPC CLASS: 424468 NO DOI FOR PATENT.
4. Scarpignato C, Pelosini I. Rifaximin, a poorly absorbed antibiotic: pharmacology and clinical potential. Chemotherapy. 2005;51 suppl 1:36–66. doi:10.1159/000081990.

5. Vaira D. Rifaximin suspension for the eradication of *Helicobacter pylori*. Curr Ther Res. 58(5):300–308.
6. Darkoh C *et al*. Bile acids improve the antimicrobial effect of rifaximin. Antimicrob agents chemother. 2010;3618–3624. doi:10.1128/AAC.00161-10.
7. Rawat S, Jain SK. Solubility enhancement of celecoxib using β-cyclodextrin inclusion complexes. Eur J Pharm Biopharm. 2004;57:263–7. doi:10.1016/j.ejpb.2003.10.020.
8. Bidyut N, Amrutansu P, Annapurna MM. Spectrophotometric estimation of rifaximin in pure and tablet dosage form. Int J Pharm Technol. 2010;2(4):1098–104.
9. Loftsson T, Vogensen SB, Desbos C, Jansook P. Carvedilol: solubilization and cyclodextrin complexation: a technical note. AAPS PharmSciTech. 2008;9(2) (# 2008). doi:10.1208/s12249-008-9055-7.
10. Patel AR, Vavia PR. Preparation and evaluation of taste masked famotidine formulation using drug/β-cyclodextrin/polymer ternary complexation approach. AAPS PharmSciTech. 2008;9(2):544–50. doi:10.1208/s12249-008-9078-0.
11. Waleczeka KJ, Cabral Marquesb HM, Hempelc B, Schmidt PC. Phase solubility studies of pure (2)-a-bisabolol and camomile essential oil with b-cyclodextrin. Eur J Pharm Biopharm. 2003;55(2):247–51. doi:10.1016/S0939-6411(02)00166-2.
12. Hirayama F, Uekama K. Cyclodextrin-based controlled drug release system. Adv Drug Deliv Rev. 1999;36:125–41. doi:10.1016/S0169-409X(98)00058-1.
13. Liu L *et al*. A study on the supramolecular structure of inclusion complex of β-cyclodextrin with prazosin hydrachloride. Carbohydrate polymers, 68(Issue 3):472–476. doi: 10.1016/j.carbpol.2006.11.007.
14. Werner F, Okemo P, Ansorg R. Antibacterial activity of East African Medicinal; plants. J Ethnopharmacol. 60:79–84.
15. Alanazi FK, El-Badry M, Ahmed MO, Alsarra IA. Improvement of albendazole dissolution by preparing microparticles using spray-drying technique. Sci Pharm. 2007;75:63–79.
16. Liu W, Wu WD, Selomulya C, Chen XD. Uniform chitosan microparticles prepared by a novel spray-drying technique. Int J Chem Eng. 2011;2011. doi:10.1155/2011/267218. Article ID 267218, 7 Pages.
17. Robinson S. (Melton Mowbray GB), Smith, Susan Stewart (Leicestershire GB). Spray-drying process for the preparation of microparticles; Application Number: 09/342356 Patent no: US 6,451,349 B1.
18. Elshafeey AH, Sami EI. Preparation and *in-vivo* pharmacokinetic study of a novel extended release compression coated tablets of Fenoterol Hydrobromide. AAPS PharmSciTech. 2008;9(3) (# 2008). doi: 10.1208/s12249-008-9135-8.
19. Narayan P, Marchant D, Wheatley MA. Optimization of spray drying by factorial design for production of hollow microspheres for ultrasound imaging. J Biomed Mater Res. 2001;56 (3):333–41. doi:10.1002/1097-4636(20010905)56:3333::AID-JBM1101>3.0.CO;2-K.
20. Tajber L, Corrigan OI, Healy AM. Spray drying of budesonide, formoterol fumarate and their composites—II. Statistical factorial design and *in vitro* deposition properties. Int J Pharm. 2009;367 (1–2):86–96. doi:10.1016/j.ijpharm.2008.09.029.